INTERNATIONAL JOURNAL OF MICROWAVE AND OPTICAL TECHNOLOGY,

VOL. 2, NO. 1, JANUARY 2007

Analysis of Frequency Behavior of Microstrip Lines on Anisotropic Substrates with Slots in Ground Plane

Sachin Singh and Banmali S. Rawat*

Department of Electrical Engineering
University of Nevada, Reno, NV 89557, U.S.A.
Tel: 17757841457, Fax: 17757846627, E- mail: rawat@ee.unr.edu

Abstract- **This paper analyzes the effects on the frequency behavior of the microstrip lines with defected ground plane structures (DGS) on anisotropic substrates. An improvement in the losses at attenuation poles and sharpness factor of LPF based on DGS on anisotropic substrates has been reported.**

Index Terms- **Defected Ground plane structure (DGS), Low pass filter (LPF), Anisotropy effects on DGS slot, Microstrip filters**

I. INTRODUCTION

Microstrip photonic band gap (PBG) structures, having periodic etched structures in the ground plane provide rejection of certain frequency bands. The difficulty in the modeling of these periodic structure lead to the investigation of a simple etched non-periodic structure in the ground plane [1]-[2]. The variation in the size of the defects changes the band gap behavior of these elements [2]. Different shapes like rectangular slots, dumb-bell slots, arrowhead slots and square head slots in the ground plane have been examined [3]. Single dimension (1-D) periodic DGS and improved exponential distribution periodic DGS based filters have also been studied [4-5]. Various microstrip low pass filters utilizing DGS elements were designed and fabricated [1]-[5]. Most of the researchers so far have examined the DGS on isotropic dielectric substrates only.

In this paper we have examined the effects of introducing dielectric substrate anisotropy on microstrip lines with DGS. The analysis is performed using 3-D finite element method based electromagnetic (EM) field simulator Ansoft HFSS (High Frequency Structure Simulator). The losses at poles are studied for the variation of W/H ratios of the microstrip line DGS based structure.

The anisotropy ratio (AR) of an anisotropic substrate has been introduced in the analysis. Improvement in losses at attenuation poles due to change in anisotropy in y-axis is reported. The improvement in sharpness factor of the filter with anisotropy variation in x-axis has been achieved. Combination of change in AR and variation in W/H has also been studied. Finally, the introduction of DGS on practical available dielectric anisotropic substrates has been examined.

II. THEORETICAL ANALYSIS AND IMPLEMENTATION OF ANISOTROPY

A simple square shaped DGS slot is shown in Fig. 1. The width of the microstrip line is w, thickness of the anisotropic substrate is h, the area of the square lattice in the ground plane is a^2, and the gap distance in the ground plane is g. The lumped equivalent circuit model of DGS (a parallel LC resonator) is shown in Fig. 1(c).

INTERNATIONAL JOURNAL OF MICROWAVE AND OPTICAL TECHNOLOGY,

VOL. 2, NO. 1, JANUARY 2007

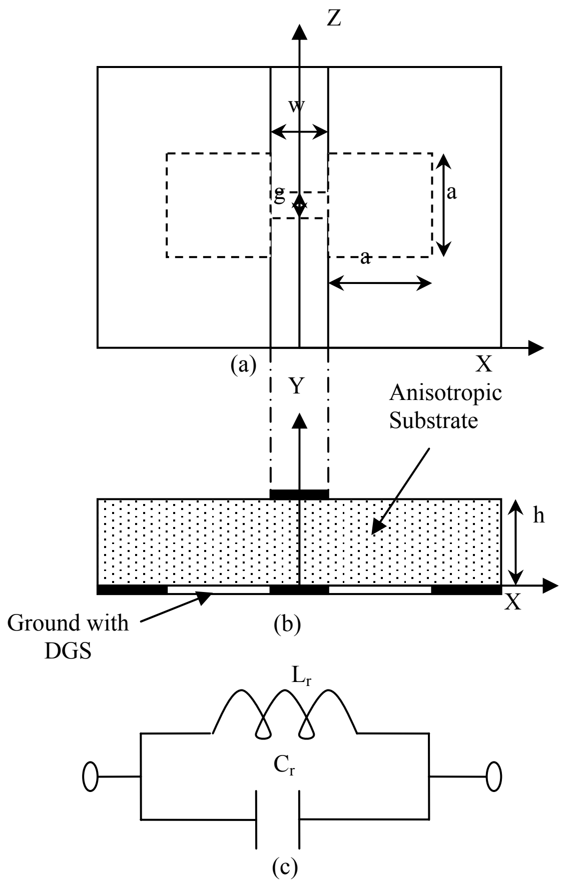

Fig.1. (a) Top view of Microstrip line with DGS. (b) Front view. (c) Equivalent circuit

There are other modeling techniques also presented by researchers [6]-[7]. Due to ease of understanding and simple modeling technique in [1]-[3], it is used in this paper. The values of the resonating inductance and capacitance L_r and C_r, respectively, are calculated as.

$$C_r = \frac{0.01 w_c}{w_0^2 - w_c^2} = \frac{0.005 f_c}{\pi (f_0^2 - f_c^2)} \qquad (1)$$

$$L_r = \frac{1}{w_0^2 C_r} = \frac{1}{4\pi^2 f_0^2 C_r} \qquad (2)$$

where ω_o is the resonance frequency (attenuation pole location) and ω_c is cut-off frequency in radians, while f_o and f_c are in Hz.

It is well understood that the substrate dielectric anisotropy reduces the difference between even and odd mode phase velocities of the coupled lines compared to isotropic or nearly isotropic substrates [8]-[10]. This in effect improves the directivity and isolation of microstrip couplers resulting in improved performance of the microstrip filters. The substrate layer considered is an anisotropic dielectric having permittivity tensor given by

$$\varepsilon = [\varepsilon] = \varepsilon_0 \begin{bmatrix} \varepsilon_{xx} & \varepsilon_{xy} & 0 \\ \varepsilon_{yx} & \varepsilon_{yy} & 0 \\ 0 & 0 & \varepsilon_{zz} \end{bmatrix} \qquad (3)$$

and the elements of the matrix are expressed as [8]

$$\begin{aligned} \varepsilon_{xx} &= \varepsilon_{zz} = \varepsilon_{\alpha\alpha}\left(\mathrm{Re}\left(e^{j\theta}\right)\right)^2 + \varepsilon_{\beta\beta}\left(\mathrm{Im}\left(e^{j\theta}\right)\right)^2 \\ \varepsilon_{yy} &= \varepsilon_{\alpha\alpha}\left(\mathrm{Im}\left(e^{j\theta}\right)\right)^2 + \varepsilon_{\beta\beta}\left(\mathrm{Re}\left(e^{j\theta}\right)\right)^2 \\ \varepsilon_{xy} &= \varepsilon_{yx} = \left(\varepsilon_{\alpha\alpha} - \varepsilon_{\beta\beta}\right)\mathrm{Re}\left(e^{j\theta}\right)\mathrm{Im}\left(e^{j\theta}\right) \end{aligned} \qquad (4)$$

where the subscripts $\alpha\alpha$ and $\beta\beta$ refer to the optical axes and θ is the anisotropy angle at which the substrate is cut with its surface to the optical axis. The anisotropy of the dielectric substrate can be transformed to its equivalent isotropic substrate [8],[10]-[13]. The transformation of dielectric anisotropic substrate to isotropic substrate is shown in the Fig.2.

INTERNATIONAL JOURNAL OF MICROWAVE AND OPTICAL TECHNOLOGY,

VOL. 2, NO. 1, JANUARY 2007

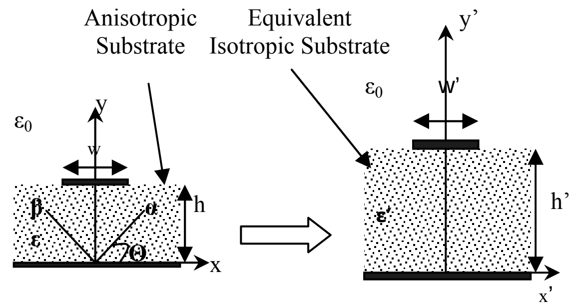

Fig. 2. Transformation of Anisotropic substrate to its Equivalent Isotropic Substrate

The equations used to transform equivalent isotropic substrate from the anisotropic substrate are given as [12].

$$\varepsilon' = \sqrt{\varepsilon_{\alpha\alpha}\varepsilon_{\beta\beta}} \qquad (5)$$

$$w' = w \qquad (6)$$

$$h' = \frac{\gamma * h}{(\gamma^2 - 1)\cos^2\theta + 1} \qquad (7)$$

where $\gamma = \sqrt{\dfrac{\varepsilon_{\beta\beta}}{\varepsilon_{\alpha\alpha}}}$.

Now, considering an anisotropic dielectric substrate with zero off diagonal anisotropy and zero anisotropy angle and using Eqs. (3)-(7), the Eqs.(5)-(7) are modified as

$$\varepsilon' = \sqrt{\varepsilon_{xx}\varepsilon_{yy}} \qquad (8)$$

$$w' = w \qquad (9)$$

$$h' = \frac{h}{\gamma} \qquad (10)$$

where $\gamma = \sqrt{\dfrac{\varepsilon_{yy}}{\varepsilon_{xx}}}$.

The transformation from anisotropic to isotropic substrate has been used in generating the simulation results using HFSS.

III. SIMULATION RESULTS

The band stop performance of the DGS slots can be controlled by the shapes and sizes of the DGS slots in the ground plane [2]-[3]. The parameters selected in this paper to characterize the band stop performance of DGS are:

(i) Width of the Microstrip line
(ii) Dielectric substrate anisotropy

The ports are matched with the characteristic impedance of the line for all the simulations. The sharpness factor (f_c/f_o) that determines the transition from pass band to stop band region, has been examined for width of the line and dielectric anisotropy variations. The maximum value of sharpness factor is 1, which provides the sharpest transition from pass band to stop band region. Also, the effects of changing width or dielectric anisotropy on the losses at the pole location and control of f_c and f_o have been investigated.

A. Effect of Variation of Microstrip Line Width

The width of the line can be used to control the parameters f_c ,f_o, L_r, C_r and the losses at the pole location for the DGS based LPF. The simulation is performed for a 62-mil thick isotropic substrate having ε_r=10, the square head DGS slot with gap g=0.2 mm, and two variations of the square lattice having a=2.5 mm and a=4.6 mm. The W/H ratio is varied from 0.1 to 3 in the steps of 0.2 by changing the width of the line. The variation of forward transmission coefficient as a function of frequency for four cases with w=0.1575 mm, 1.5 mm, 3.3075 mm and 4.725 mm is shown in Fig. 3 for a=2.5 mm. The results

INTERNATIONAL JOURNAL OF MICROWAVE AND OPTICAL TECHNOLOGY,

VOL. 2, NO. 1, JANUARY 2007

obtained for w=1.5 mm or w/h=0.95 are in good agreement with the result obtained by [2].

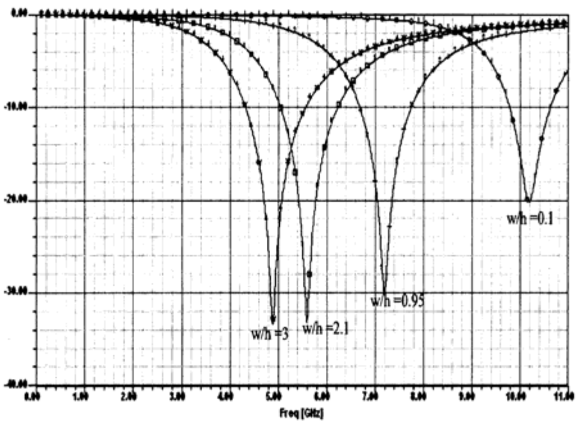

Fig. 3. Forward Transmission coefficient for a=2.5mm for different w/h ratio.

With the increase in W/H ratio, the f_c and f_o values are reduced and the losses at the pole location are increased as shown in Fig. 3. The frequency behavior for each and every variation of W/H is simulated but due to space limitation, these frequency behavior plots are not included. The values of equivalent L_r and C_r are extracted using equation (1) and (2), the f_c and f_o values are taken from the simulated results. The variations of the losses at the poles for two dimensions of square head against W/H ratio are shown in the The change in the sharpness factor with respect to W/H ratio is shown in Fig.5.

The variation of DGS characteristics with W/H are tabulated in Table 1. The row 2 of the table, shows the change in cut off frequency f_c, by varying W/H ratio from 0.1 to 3, for a=2.5 mm and a=4.6 mm. In the first cell of the Table 1, f_c varies from 9.1 GHz for W/H=0.1 to 3.5 GHz for W/H=3. Similarly, equivalent capacitance reduces form 0.71 pF at W/H=0.1 to 0.48 pF at W/H=3 when the square lattice dimension is a=2.5 mm.

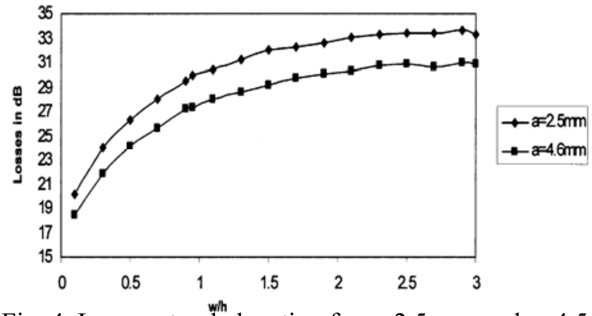

Fig. 4. Losses at pole location for a=2.5 mm and a=4.5 mm against the W/H ratio.

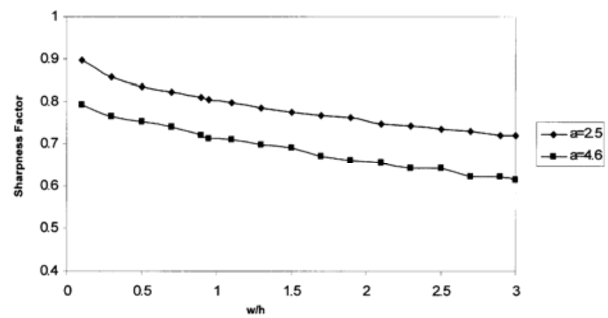

Fig. 5. Sharpness factor for a=2.5 mm and a=4.5 mm against the W/H ratio.

Table 1: Characteristics of DGS slots for dimensional variation of W/H from 0.1 to 3

Variations in	a=2.5 mm	a=4.6mm
f_c (GHz)	9.1-3.5	5.2-2
f_o (GHz)	10.2-4.8	6.6-3.3
C_r (pF)	0.71-0.48	0.51-0.47
L_r (nH)	0.34-2.17	1.14-4.81

The variation in C_r is 0.23 pF for a=2.5 mm and 0.04pF for a=4.6 mm. The variation of L_r is 1.83 nH for a=2.5mm and 3.67 nH for a=4.6 mm. The results are in agreement with the results shown in [2], that the series inductance is controlled by changing the dimensions of the square head.

The value of L_r due to DGS slots increases whereas the C_r decreases with W/H as seen from Table 1. The surface area of the defect in the ground plane increases with W/H, which increase the shield current density on ground plane. This results in increase of the equivalent inductance with W/H. In Fig. 4, the losses at pole increase with increase in W/H ratio but start reaching a steady state at higher ratios. The increase in shield current density, due to increase in the W/H ratio increases the ohmic losses which results in the increase of losses. Also, in Fig. 5, the sharpness factor starts decreasing with W/H ratio and reaches steady state with higher ratio. As the parallel equivalent circuit behaves like an inductor at any frequency lower than the resonance frequency [3], the cutoff frequency of the circuit becomes dependent on the value of the equivalent inductance. The change in equivalent capacitance is lower than that of inductance and the resonant frequency depends upon both the reactive elements. Therefore, the reduction in f_o is less as compared to the reduction in f_c with increase in the W/H ratio. This results in decrease of sharpness factor. We have seen in this section that, by varying W/H ratio, the losses at poles, the sharpness factor and other characteristics of the DGS slots can be controlled.

B. Effect of Substrate Dielectric Anisotropy

The substrate dielectric anisotropy is changed in two ways and this change in dielectric constant is defined in terms of Anisotropy Ratio (AR). When the dielectric anisotropy is changed along the x-axis of the substrates, we define the anisotropy ratio AR_x as

$$AR_x = \frac{\varepsilon_x}{\varepsilon_y} \qquad (11)$$

In this case, the anisotropy is changed by varying dielectric constant in x-axis and keeping it constant in the y-axis. Similarly, when the dielectric constant is changed in y-axis and is kept fixed in x-axis, the anisotropy ratio is defined as

$$AR_y = \frac{\varepsilon_y}{\varepsilon_x} \qquad (12)$$

The effects of changing these anisotropies on the characteristics of DGS slot are analyzed in this subsection.

a) Variation of Anisotropy ratio for 50 Ohm line

The anisotropy ratio is changed for a 50 ohm line on a substrate with h=62 mil, ε_r=10, g=0.6 mm and a=4.6 mm. The variation in AR is done from 0.5 to 5 with steps of 0.5 and from 5 to 9 with steps of 1. The results obtained by changing AR_y are shown in Fig 6. These simulation results are for AR_y=1, 3, 6 and 9.

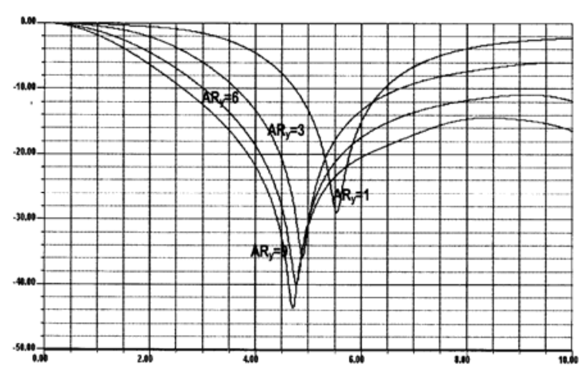

Figure 6: Forward Transmission coefficient for different AR_y ratio.

The losses at poles are improved with AR_y as be shown in Fig. 6. However, the sharpness factor

INTERNATIONAL JOURNAL OF MICROWAVE AND OPTICAL TECHNOLOGY,

VOL. 2, NO. 1, JANUARY 2007

decreases as shown in Fig. 8. The frequency behavior for variation of AR_y was simulated and then the results were extracted, and for the sake of brevity, all the simulation results are not shown. Similarly, the simulation for the variation of AR_x was done and the results for f_c ,f_o, L_r, C_r and losses at poles are extracted from these simulation results. In Fig. 7, it is seen that by changing AR_x, losses at poles are decreased, but the variation is not as much as in the case of AR_y, whereas the sharpness factor is improved as shown in Fig. 8. The change in f_c ,f_o, L_r, and C_r due to variations in AR_x and AR_y are shown in Table 2.

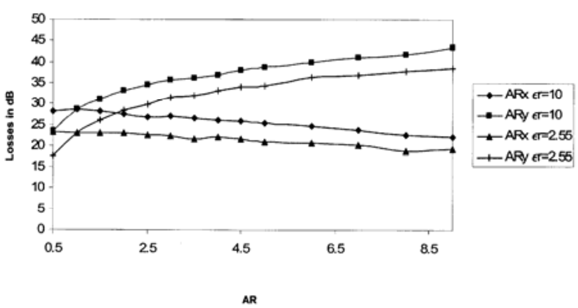

Figure 7: Losses at pole location for different anisotropy ratio for a 50 0hm line (ε_r =10 and ε_r =2.55)

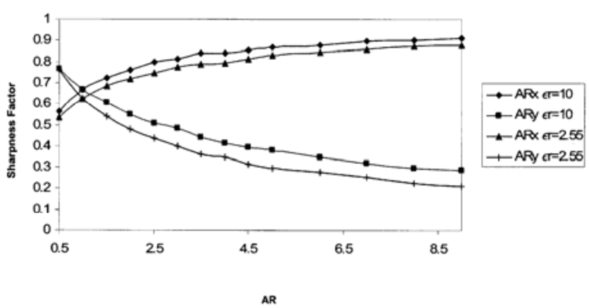

Figure 8: Sharpness factor for different anisotropy ratio for a 50 0hm line (ε_r =10 and ε_r =2.55).

Table 2: Characteristics of DGS slots for anisotropic variation (ARx and ARy) from 0.5 to 9 for 50 ohm line (εr =10 and εr =2.55)

	ε_r =10		**ε_r =2.55**	
Variation in	AR_x	AR_y	AR_x	AR_y
f_c (GHz)	3.8-2.4	4.6-1.3	4.1-3.4	5.5-1.2
f_o (GHz)	6.8-2.6	6-4.7	7.7-3.8	7.2-5.9
C_r (pF)	0.19-3.16	0.49-0.1	0.16-1.59	0.39-0.06
L_r (nH)	2.86-1.14	1.44-10.92	2.77-1.06	1.24-12.17

The cut off frequency f_c is reduced from 3.8 GHz to 2.4 GHz as the AR_x is increased from 0.5 to 9. Simulations were also done for 50 ohm line on a substrate with h=62 mil, ε_r=2.55, g=0.6mm and a=4.6mm. The extracted results obtained for the losses at poles and sharpness factor against anisotropy ratio are also shown in Fig. 7 and Fig. 8, respectively. The change in f_c ,f_o, L_r, and C_r due to variations in AR_x and AR_y for ε_r=2.55 are tabulated in Table 2. The results show similar pattern as shown by the 50 ohm line on a dielectric substrate of dielectric constant ε_r=10.

The variation in f_c can be largely controlled by varying AR_y, whereas f_o can be controlled by controlling AR_x as shown in Table 2. Similarly, the equivalent capacitance is controlled by controlling AR_x and inductance by AR_y. The effective inductance decreases with AR_x but increases with AR_y. As explained earlier in Section III A the W/H changes the effective inductance and capacitance of the DGS. Essentially, by varying anisotropy ratio the W/H ratio is varied as can be seen from equations (8) to (10). So, when AR_x increases, it lowers the W/H ratio and in effect decreases the effective inductance. Similarly when AR_y increases, it increases the W/H ratio and in turn increases the effective inductance.

INTERNATIONAL JOURNAL OF MICROWAVE AND OPTICAL TECHNOLOGY,

VOL. 2, NO. 1, JANUARY 2007

b) Variation of AR and W/H

In this subsection both the width of the line and anisotropy ratio are varied. The variations in W/H ratio considered for simulations are 0.1, 1 and 3, whereas the two types of AR are varied from 1 to 5 with a step of 0.5. These variations are done for a microstrip line on a substrate with h=62 mil, ε_r=10, g=0.6mm and a=4.6mm. The results for losses at poles for different W/H ratios are shown in Fig. 9 and sharpness factor in Fig. 10 for variation in AR_x and AR_y. The change in f_c ,f_o, L_r, and C_r due to variations in AR_x and due to AR_y for different W/H ratios are given in Table 3.

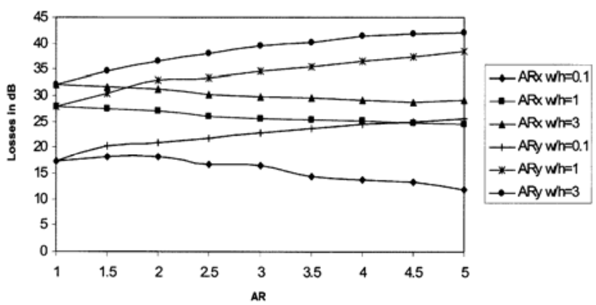

Figure 9: Losses at pole location for anisotropy ratio AR_x and AR_y for different w/h line (ε_r =10).

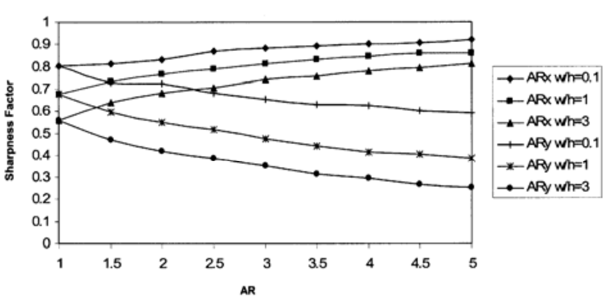

Figure 10: Sharpness factor for anisotropy ratio AR_x and AR_y for different w/h line (ε_r=10).

The anisotropy ratio and W/H are also varied for a microstrip line on a substrate with h=62 mil, ε_r=2.55, g=0.6mm and a=4.6mm. Results for losses at poles for different w/h are shown in Fig. 11 and sharpness factor in Fig. 12 with the variation in AR_x and AR_y. The change in f_c ,f_o, L_r, and C_r due to variations in AR_x and due to AR_y for different w/h are shown in Table 3.

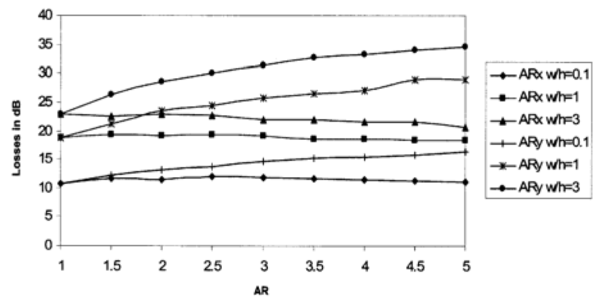

Figure 11: Losses at pole location for anisotropy ratio AR_x and AR_y for different w/h line (ε_r =2.55).

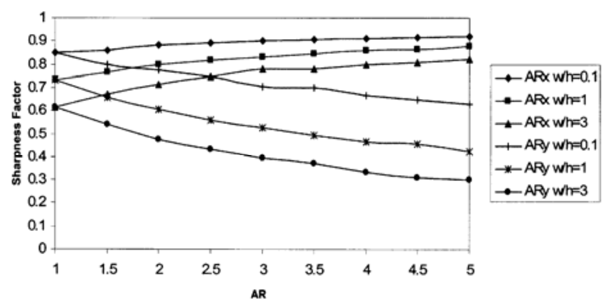

Figure 12: Sharpness factor for anisotropy ratio AR_x and AR_y for different w/h line (ε_r=2.55).

The variation in AR_x reduces the losses at poles, whereas the variation in AR_y increases the losses at poles. Also, the variation of losses due to change in AR_x is not as high as due to AR_y as seen in Fig. 9 and Fig. 11. Also, the losses at poles are increased with W/H, which is in agreement with the findings in Section III A, where the line width is varied. Again, the sharpness factor improves with AR_x and decreases with AR_y. Also, the sharpness factor becomes lower for higher W/H ratio as seen in

Fig. 10 and Fig .12. It is noted, from Table 3, that f_c and L_r are better controlled by AR_x and f_o and C_r are better controlled by AR_y. Also, with W/H the location of f_c and f_o can be controlled. The results of this subsection agree well with that of the previous subsections.

Table 3: Characteristics of DGS slots for anisotropic variation (ARx and ARy) from 1 to5 for different w/h line (εr =10 and εr=2.55)

w/h=0.1				
	ε_r =10		ε_r=2.55	
Variation in	**AR_x**	**AR_y**	**AR_x**	**AR_y**
f_c (GHz)	5.7-3.6	5.7-3.7	9.4-6.8	9.4-6.5
f_o (GHz)	7.1-3.9	7.1-6.3	11-7.4	11-10.4
C_r (pF)	0.51-2.38	0.51-0.23	0.45-1.29	0.45-0.16
L_r (nH)	1-0.68	1-2.79	0.47-0.35	0.47-1.48
w/h=1				
	ε_r =10		ε_r=2.55	
Variation in	**AR_x**	**AR_y**	**AR_x**	**AR_y**
f_c (GHz)	3.8-2.9	3.8-1.9	6.6-5.3	6.6-3.5
f_o (GHz)	5.6-3.3	5.6-4.9	9-6	9-8.2
C_r (pF)	0.35-1.6	0.35-0.15	0.28-1	0.28-0.1
L_r (nH)	2.3-1.44	2.3-7.23	1.13-0.69	1.13-3.8
w/h=3				
	ε_r =10		ε_r=2.55	
Variation in	**AR_x**	**AR_y**	**AR_x**	**AR_y**
f_c (GHz)	2.3-2	2.3-0.9	4.1-3.7	4.1-1.8
f_o (GHz)	4.2-2.4	4.2-3.7	6.7-4.5	6.7-6.1
C_r (pF)	0.31-1.55	0.31-0.12	0.24-0.89	0.24-0.08
L_r (nH)	4.7-2.7	4.7-15.8	2.4-1.4	2.4 -8

c) Practical Anisotropic Substrate

In this section, three of the available anisotropic substrates are considered and their results are compared with that of their isotropic counterpart [14]. The three anisotropic substrates considered for the analysis are:

(i) Epsilam-10

The dielectric constant of anisotropic epsilam-10 is $\varepsilon_x= \varepsilon_z =13$; $\varepsilon_y=10.3$ and that of Isotropic epsilam-10 is $\varepsilon_x= \varepsilon_z =\varepsilon_y=10.3$. In Epsilam-10, the variation in anisotropy is in x-axis therefore the anisotropy ratio variation is of the form of AR_x. And, from the analysis so far, it can be predicted that the variation of losses at poles is not affected much, but the sharpness factor is improved. The results shown in Fig. 13 and Fig. 14 agree well with the prediction. The change in f_c ,f_o, L_r, and C_r due to variations in W/H for Anisotropic and its Isotropic Epsilam-10 counterpart are given in Table 4. The equivalent capacitance of Anisotropic Epsilam-10 is higher than that of its Isotropic counterpart, but the equivalent inductance for anisotropic Epsilam-10 is lower than that for Isotropic Epsilam-10.

(ii) Pyrolitic Boron Nitride (PBN)

The dielectric constant of anisotropic PBN is $\varepsilon_x= \varepsilon_z =5.12$; $\varepsilon_y=3.45$ and that of Isotropic PBN is $\varepsilon_x= \varepsilon_z =\varepsilon_y=3.45$. PBN also has the variation in anisotropy in the x-axis, similar to Epsilam-10; therefore the anisotropy ratio variation is of the form of AR_x. Again, it can be predicted that the variation of losses at poles is not affected much, but the sharpness factor improves. The results shown in Fig. 13 and Fig. 14 agree with this prediction. The change in f_c, f_o, L_r, and C_r due to variations in W/H for Anisotropic and its Isotropic PBN counterpart are given in Table 4. The equivalent capacitance of Anisotropic PBN is higher than that of its Isotropic counterpart, but the equivalent inductance of anisotropic PBN is lower than that of isotropic counterpart.

INTERNATIONAL JOURNAL OF MICROWAVE AND OPTICAL TECHNOLOGY,

VOL. 2, NO. 1, JANUARY 2007

(iii) Sapphire

The dielectric constant of anisotropic Sapphire is $\varepsilon_x= \varepsilon_z =9.4$; $\varepsilon_y =11.6$ and that of Isotropic Sapphire is $\varepsilon_x= \varepsilon_z =\varepsilon_y=9.4$. Sapphire has the variation of dielectric in y-axis therefore AR variation is of the form of AR_y. So, it can be predicted that there is improvement of losses at poles with anisotropy, whereas the sharpness factor is reduced. The results shown in Fig. 13 and Fig. 14 agree with this prediction. The change in f_c, f_o, L_r, and C_r due to variations in w/h for Anisotropic and its Isotropic Sapphire counterpart are given in Table 4. The equivalent inductance of Anisotropic Sapphire is higher than that of its Isotropic counterpart, but the equivalent capacitance of anisotropic sapphire is lower than that of isotropic counterpart.

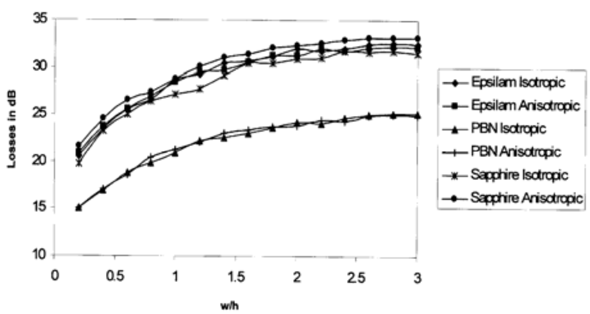

Figure 13: Losses at pole location for Isotropic and Anisotropic Epsilam-10 against w/h ratio.

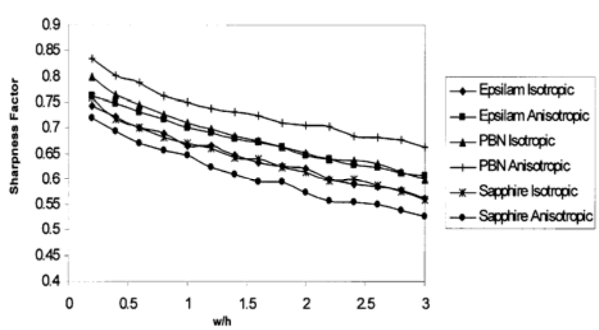

Figure 14: Sharpness factor for Isotropic and Anisotropic Epsilam-10 against w/h ratio.

Table 4: Characteristics of DGS slots for different practical anisotropic substrates and their counterpart isotropic substrate for different w/h variations

	EPSILAM-10		**PBN**		**SAPPHIRE**	
Variations in	**Aniso-tropic**	**Isotro-pic**	**Aniso-tropic**	**Isotro-pic**	**Aniso-tropic**	**Isotro-pic**
f_c GHz	4.9-2.3	5.1-2.3	7.5-3.7	7.9-3.7	5-2.2	5.4-2.4
f_o GHz	6.4-3.8	6.8-4.1	9-5.6	9.9-6.1	7-4.1	7.1-4.2
C_r (pF)	0.46-0.41	0.39-0.32	0.48-0.34	0.36-0.24	0.34-0.28	0.4-0.31
L_r (nH)	1.37-4.41	1.41-4.78	0.65-2.43	0.74-2.78	1.53-5.27	1.25-4.62

IV. CONCLUSION

In this paper, we have shown that the characteristics of the DGS slots can be controlled by changing the width of the line, AR of the substrate. Also, we have shown that the losses at the poles can be increased by changing the AR in y-axis and sharpness factor is improved by changing the AR in x-axis. The concept developed in the analysis has been applied to the practical anisotropic substrate, and the results obtained agreed well with the concept. The theoretical findings of this paper have been experimentally verified by these authors [15].

ACKNOWLEDGEMENT

The authors would like to acknowledge ANSOFT HFSS for their support of the simulation software HFSS V 9.

REFERENCES

[1] Jong-Im Park, Chul-Soo Kim, Juno Kim, Jun-Seok Park, Yongxi Qian, Dal Ahn and Itoh, T., “Modeling of a photonic bandgap and its application for the low-pass filter design,” *1999 Asia Pacific Microwave Conference*, Singapore, APMC’99, vol. 2 , 30 Nov.-3 Dec. 1999, pp. 331 - 334.

[2] D. Ahn, J.-S. Park, C.-S. Kim, J. Kim, Y. Qian and T. Itoh, “A design of the low-pass filter using the novel microstrip defected ground structure,” *IEEE Trans. Microwave Theory and Tech.*, vol. 49, pp. 86 – 93, Jan. 2001.

[3] A.B. Abdel-Rahman,. A.K. Verma,. A. Boutejdar, and A.S. Omar, “Control of bandstop response of Hi-Lo microstrip low-pass filter using slot in ground plane,” *IEEE Trans. Microwave Theory and Tech.*, vol. 52, pp. 1008– 1013, Mar. 2004.

[4] Chul-Soo Kim, Jun-Seok Park, Dal Ahn and Jae-Bong Lim, “A novel 1-D periodic defected ground structure for planar circuits,” *IEEE Microw. Guided Wave Lett.*, vol. 10 , pp. 131 – 133, Apr. 2000.

[5] Hai-Wen Liu, Zheng-Fan Li, Xiao-Wei Sun and Jun-Fa Mao, “An improved 1D periodic defected ground structure for microstrip line,**”** *IEEE Microw. Guided Wave Lett.*, vol. 14, pp. 180- 182, Apr. 2004.

[6] Jun-Seok Park, Jae-Ho Kim, Jong-Hun Lee, Sang-Hyuk Kim and Sung-Ho Myung, “A novel equivalent circuit and modeling method for defected ground structure and its application to optimization of a DGS lowpass filter,**”** *IEEE MTT-S Int. Microwave Symp. Dig.*, vol. 1, 2-7 Jun. 2002, pp. 417 – 420.

[7] Haiwen Li, Xiaowei Sun and Zhengfan Li, “A new parameter extraction method for DGS and its application to the Low-Pass Filter,” Active and Passive Elec. Comp., vol. 27, pp. 119-123, Jun. 2004.

[8] Lukang Yu, and Banmali Rawat, “Quasi-static analysis of three-line microstrip symmetrical coupler on anisotropic substrates,” *IEEE Trans. Microwave Theory and Tech.*, vol. 39, pp. 1433-1437, Aug. 1991.

[9] N.G.Alexopoulos, and C.M. Krowne,., “Characteristics of single and coupled microstrips on anisotropic substrates,” *IEEE Trans. Microwave Theory and Tech.*, vol. 26, pp. 387 – 393, Jun. 1978.

[10] M. Kobayashi, and R. Terakado, “Method for equalizing phase velocities of coupled microstrip lines by using anisotropic substrate,” *IEEE Trans. Microwave Theory and Tech.*, vol. 28, pp. 719 – 722, Jul. 1980.

[11] M. Horno,., “Calculation of quasi-static characteristics of microstrip on anisotropic substrate using mapping method,” *IEEE MTT-S Int. Microwave Symp. Dig.*, vol. 80, May 1980, pp. 450 - 452.

[12] Masanori Kobayashi, and Ryuiti Terakado, , “New view on anisotropic medium and its application to transformation from anisotropic to isotropic problems,” *IEEE Trans. Microwave Theory and Tech.*, vol. 27, pp. 769-775, Sep. 1979.

[13] M. Horno, “Quasistatic characteristics of covered coupled microstrips on anisotropic substrates: spectral and variational analysis,” *IEEE Trans. Microwave Theory and Tech.*, vol. 82, pp. 1888 – 1892, Nov. 1982.

[14] E. Drake, R. R. Boix, Horno, M. and Sarkar, T. K., “Effect of substrate dielectric anisotropy on the frequency behavior of microstrip circuits,” *IEEE Trans. Microwave Theory and Tech.*, vol. 48, pp. 1394-1403, Aug. 2000.

[15] Sachin Singh, and Banmali Rawat, “Improved performance of DGS based LPF using anisotropic substrate,” *International Journal of Microwave and Optical Technology,* Vol. 1, No.1, pp. 28-34, June 2006. (Invited Paper).